

Detection Performance of Compressive Sensing Applied to Radar

Laura Anitori^{1,2}
and Matern Otten¹

¹TNO Defence, Safety and Security
The Hague, The Netherlands
Email: laura.anitori@tno.nl

Peter Hoogeboom^{1,2}

²International Research Center
for Telecommunications and Radar (IRCTR)
Technical University of Delft
Delft, The Netherlands

Abstract—In this paper some results are presented on detection performance of radar using Compressive Sensing. Compressive sensing is a recently developed theory which allows reconstruction of sparse signals with a number of measurements much lower than implied by the Nyquist rate. In this work the behavior of detection and false alarm performance of a CS based radar using a stepped frequency waveform is analyzed. The results are obtained via simulations with known noise levels for several different scenarios (e.g. single and multiple targets, varying compression factors and Signal to Noise Ratios (*SNR*)). Performance of CS reconstruction and detection are analyzed by means of Receiver Operating Characteristic (ROC) curves and compared to conventional Matched Filtering.

I. INTRODUCTION

Compressive Sensing (CS) is a novel data acquisition/processing method which allows reconstruction of sparse signals with a number of measurements much lower than what is implied by the Nyquist rate. Because of the wide range of applications, this topic has attracted the interest of many researchers in the last few years. Although the field of CS has been developed only recently, the theory behind it is widely documented in literature, see [1]–[6] and references therein, and CS has been already successfully demonstrated in several fields of research, such as communications, optical and medical imaging, sensor networks, remote sensing and radar.

In radar systems increasing demands in terms of resolution (bandwidth), and trends towards multi-channel radar systems, keep increasing the required sampling rates and amounts of data to be handled. In radar, the covered space is often divided into range and Doppler cells, and sometimes azimuth and elevation cells, which typically contain a number of targets much smaller than the number of cells in the coverage area. This spatial sparseness can be exploited to reduce the requirements on sampling and data rates, or to reduce the number of physical sensors in the acquisition system, or to improve resolution with equal amount of measurements. Recent examples of Compressive Sensing applied to radar were provided in e.g. [7]–[13].

However, while classical radar detection theory has since long been firmly established, detection properties of CS based approaches are not yet very well known. Moreover, a new set of parameters which do not appear in conventional radar

systems, such as compression factor (δ), target sparseness (K) and reconstruction threshold (σ_{bpdn}) influence the final detection probability. These parameter values must either be estimated from the compressed measurements or set by the user based on prior knowledge and a trade off between output target/noise power and data reduction.

In the design phase of a radar using a CS architecture the system engineer would have to make choices on the minimum number of measurements required to achieve a desired false alarm/detection probability (P_{fa}, P_d) based on an expected dynamic range. Furthermore, in an adaptive scheme, such as a Constant False Alarm Rate (CFAR) detector, the way to set both the CS reconstruction threshold and the CFAR threshold must be established.

The goal of this work is to understand the effects of all parameters (separately and jointly) on the detection performance of a CS based radar, so that a good trade off can be achieved between data reduction and detection capability. To this end, an analysis is carried out by simulations of the Receiver Operating Characteristic (ROC) of a CS based radar for several sets of parameters (δ, K, σ_{bpdn}) and input Signal-to-Noise Ratios (*SNR*) assuming the noise power to be known. From the ROC curves a power budget graph is derived, which can be used in the design phase of a CS radar. Also, the possibility of performing coherent integration after CS reconstruction is investigated here. The results obtained using Compressive Sensing are compared to conventional Matched Filter (MF) processing followed by detection.

II. COMPRESSIVE SENSING FRAMEWORK

Suppose that a signal vector \mathbf{x} of length N needs to be observed, and assume that there exists a known basis in which the signal is K sparse (or compressible), i.e. $\mathbf{x} = \Psi\alpha$ and only K coefficients in α are non-zero. If this condition is satisfied, then the signal vector \mathbf{x} can be reconstructed from a number of measurements $M \ll N$. The measurement vector \mathbf{y} is given by

$$\mathbf{y} = \Phi\mathbf{x} + \mathbf{n} = \Phi\Psi\alpha + \mathbf{n} = \Theta\alpha + \mathbf{n} \quad (1)$$

where Φ is the $M \times N$ sensing matrix and \mathbf{n} is white Gaussian noise with variance σ^2 .

Given the fact that \mathbf{x} is K sparse in the known domain Ψ , the theory of CS guarantees that in the absence of noise the

original observation vector \mathbf{x} can be reconstructed "perfectly with overwhelming probability" from a number of measurements \mathbf{y} which is of the order [3] $M \geq C\mu^2(\Psi, \Phi)K \log(N)$, where $\mu(\Psi, \Phi)$ is defined as the coherence between the sensing matrix Φ and the sparsity basis Ψ (i.e. the largest correlation between all possible pairs of columns of the two matrices) and C is a constant. Examples of incoherent pairs are, e.g. random sensing matrices with any sparsity matrix, or time and Fourier (which will be used later in this paper).

Since the number of measurements M is much smaller than the number of coefficients N that need to be reconstructed, the problem is ill-posed. However, if the matrix Θ satisfies the Restricted Isometry Property (RIP), [15], then CS theory suggests that the sparse vector α can be recovered by choosing, amongst all solutions, the one with minimum l_1 norm which is in agreement with the measured data, i.e.

$$\hat{\alpha} = \underset{\alpha}{\operatorname{argmin}} \|\alpha\|_1 \quad \text{s.t.} \quad \|\Theta\alpha - \mathbf{y}\|_2 \leq \sigma_{bpdn} \quad (2)$$

where σ_{bpdn} is a threshold proportional to the noise standard deviation. Equation (2) is a convex program known as Basis Pursuit Denoising (BPDN), [5]. A number of equivalent formulations of equation (2) can be found in the literature, [5]- [16]. In the results presented here the Spectral Projected Gradient method proposed in [14] was used to solve equation (2).

A. Signal Model

In the work presented here, the case of a one dimensional radar is considered. The problem in this case is determining the presence or absence of a target in a given range bin when the compressed received signal is corrupted by additive Gaussian noise. To perform CS in range it is assumed that the transmitted waveform consists of simultaneously transmitted discrete frequencies¹. After reception and demodulation each range bin maps to a phase which is linear in the transmitted frequency, over the whole transmitted bandwidth.

To apply Compressive Sensing, the number of discrete frequencies which are transmitted is reduced from N (which represents the Nyquist rate for unambiguous mapping of ranges to phases over the whole bandwidth) to M , with $M \ll N$, where the selected M frequencies are chosen uniformly at random. Furthermore, it is assumed that the same total power is transmitted, irrespective of the number of selected frequencies, in order to achieve a 'fair' comparison from a system point of view.

Using this signal model the equivalent sensing matrix Φ is an incomplete Fourier matrix of the form:

$$\Phi = \frac{1}{\sqrt{M}} \begin{bmatrix} e^{-ik_1 r_1/N} & \dots & e^{-ik_1 r_N/N} \\ \vdots & \ddots & \vdots \\ e^{-ik_M r_1/N} & \dots & e^{-ik_M r_N/N} \end{bmatrix} \quad (3)$$

where $k_m = k_0 + m 2\pi/\Delta R$, $m = 1, \dots, M$ is the wave number, with $\Delta R = r_N - r_0$, and $r_n = r_0 + n \delta R$, $n = 1, \dots, N$ is the range bin index, with $\delta R = \Delta R/N$.

Throughout the simulations \mathbf{x} is a length N sparse vector containing the K complex target amplitudes a_k , $k = 1, \dots, K$, at indices corresponding to range bins where the targets are located and zeros elsewhere, i.e. $\mathbf{x} = [a_1, 0, 0, a_2, \dots, 0, a_K]$. This means that the sparsity domain Ψ is the range (time) domain itself, i.e. Ψ is the canonical basis \mathbf{I}_N and therefore Ψ and Φ are maximally incoherent.

For comparison also the Matched Filter and the Decimated Matched Filter (DMF) were simulated. DMF is obtained just like a conventional matched filter, but with the same number M of samples as in the CS case. Thus the DMF is a filter matched to the compressed set of frequencies².

B. Signal to Noise Ratio (SNR)

Define the input Signal-to-Noise Ratio (SNR_{in}) for each target respectively as

$$\begin{aligned} SNR_{in} &= |a_k|^2 / N \sigma^2 & \text{MF} \\ SNR_{in} &= |a_k|^2 / M \sigma^2 & \text{DMF, CS} \end{aligned} \quad (4)$$

where σ^2 is the noise variance per sample.

The dependence of SNR_{in} from N or M is a consequence of the assumption of constant transmitted power. However, it is the filter output SNR, i.e. the input SNR to the detector, that determines detection probability (P_d) and False Alarm Probability (P_{fa} or FAP), and so for ROC based comparison it is appropriate to obtain an output SNR independent of M or N . With the above definition of input SNR , the output SNR for both MF and DMF is given by³

$$SNR_{out} = |a_k|^2 / \sigma^2 \quad \text{MF, DMF} \quad (5)$$

and it is independent of M or N .

III. RECEIVER OPERATING CHARACTERISTIC (ROC) CURVES

As mentioned in the introduction, while classical radar detection theory is well established, detection properties of CS based approaches are not yet very well known. Moreover if one wishes to design a CS based radar, several parameters come into play. The first question would be how to select M and how to set the threshold σ_{bpdn} in equation (2) to achieve a desired (P_d , P_{fa}) with an assigned SNR . Another question of interest is whether or not a detector should be used after

¹As described in [7], in an operational system no frequency samples would be thrown away but rather the available power would be equally divided over the reduced set of M frequencies. While two types of waveforms are proposed in [7], namely non-uniform stepped frequency and simultaneous transmission of frequencies, the latter requires a lower sampling rate and therefore would be preferred in an actual implementation. However from the signal model point of view there is no difference between the two schemes.

²Note that for conventional Matched Filtering the sensing matrix is a complete Fourier matrix of size $N \times N$ with normalization factor $1/\sqrt{N}$ while for DMF the sensing matrix is the same as in equation (3), i.e. the output of the DMF is given by $\hat{\mathbf{x}}_{DMF} = \Phi^H \mathbf{y}$

³For CS it is not common to define an output SNR , since the CS solution is non-linear.

CS reconstruction, as shown in figure 1, or if the non-zero samples in $\hat{\mathbf{x}}$ should already be considered as detections. More specifically, the question is whether it is possible to optimize (P_d , P_{fa}) by only choosing σ_{bpdn} properly (i.e., $\eta = 0$ in figure 1) or if it is better to use a second detection block (i.e., $\eta \neq 0$).

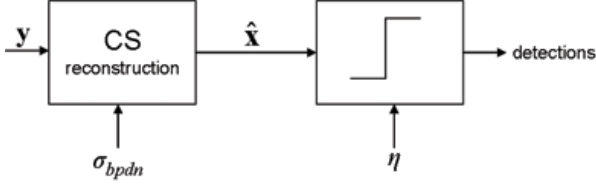


Fig. 1. Model used for generating ROC curves. The case $\eta = 0$ corresponds to considering the CS reconstructed samples as detections.

Equation (2) suggests that the value of σ_{bpdn} should be proportional to the actual noise standard deviation σ , although the constant of proportionality is not known. From simulation results it appears that the optimum value (in terms of ROC) of σ_{bpdn} is also related to M and N , and smaller values of σ_{bpdn} give better performances for smaller M .

To answer the above questions and to compare the performance of CS with MF and DMF, ROC curves were evaluated for several sets of the parameters σ_{bpdn} , SNR , M , and number of targets K . Note that the FAP is computed over all output samples except the target samples with 2 guard cells margin. For each set of parameters 10000 Monte Carlo simulations were performed and results are compared on the basis of an equal MF output SNR . For the case of a single target $N = 200$ was used and $M = 10, 20, 30, 40, 50$, and 66 , while for the case of 5 targets N was set equal to 1000 and $M = 50, 100, 150, 200, 250$, and 330 . For the selected values of M and N the ratios $\delta = M/N$ and $\rho = K/M$ are constant for both values of K and equal to $\delta = [0.05, 0.1, 0.15, 0.2, 0.25, 0.33]$ and $\rho = [0.1, 0.05, 0.033, 0.025, 0.02, 0.0152]$. Having constant ratios for different number of targets allows to compare the results in a consistent way, e.g. δ or ρ can be selected equal for both target scenarios and only look at variations of (P_d , P_{fa}) versus K .

The range of values of SNR_{out} is, for both target scenarios, between -2 and 15 dB. Values outside this range were simulated as well [17], but not reported here, as they are of less interest, since detection is either impossible (low SNR) or almost certain (high SNR). The simulated targets are point targets with constant amplitude. For each SNR_{out} , ROC curves were evaluated for set of values of σ_{bpdn} proportional to σ and, for varying M , the ratio σ_{bpdn}/σ was kept constant and equal to 2, 4, 6 and 8 for the single target case and $\sigma_{bpdn}/\sigma = 4, 8, 13, 15$ and 18 for the case of 5 targets. For comparison the results obtained using $\sigma_{bpdn} = 0$ are also reported here. In figure 2 an example of ROC curves for 1 target is shown, for $M = 66$ and $SNR_{out} = 12$ dB. To obtain this figure a second detector was used after CS reconstruction, with varying detection threshold η to obtain the ROC curves. The case in which the CS reconstructed signal samples would

be considered already as detections is a special case of the model in figure 1 (i.e. $\eta = 0$), and is shown in the figure with a square, the color of which corresponds to a given σ_{bpdn} , as shown in the legend. For this last case in fact one does not obtain a ROC curve but a single point, since after CS reconstruction P_d and P_{fa} cannot be controlled anymore. In figure 2 the solid lines are ROC corresponding to the case of CS plus detector (i.e. $\eta \neq 0$) for a few values of the CS threshold σ_{bpdn} . From the simulated ROC plots it appears that using CS followed by a separate detector, one can achieve better performance than in the $\eta = 0$ case, especially since tuning η allows to reduce FAP while maintaining a high P_d . Moreover, although the optimum threshold σ_{bpdn} in terms of ROC changes slightly for each value of M (and independently of SNR), it is important to notice that for a suboptimum value of the threshold (e.g. $\sigma_{bpdn}/\sigma = 2$ or 4 in figure 2) performance degrade gracefully. This behavior suggests that in an adaptive scheme estimation errors on the noise level could be well tolerated, unless of course the noise power is overestimated (which could happen for example at high input SNR) and all reconstructed samples would be zero because σ_{bpdn} is too high.

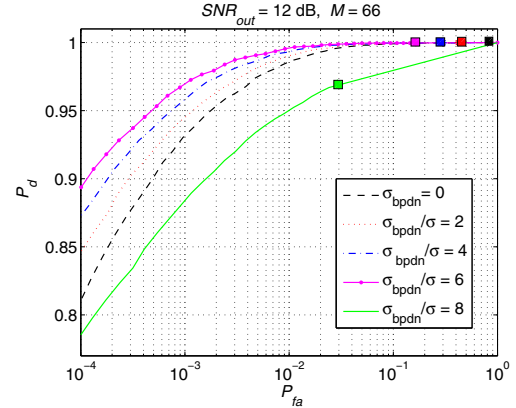


Fig. 2. P_d versus P_{fa} (ROC) for $SNR = 12$ dB and a single target. $M = 66$.

An overview of CS performance compared to MF and DMF is shown in figure 3. Here P_d is plotted versus SNR for a fixed $P_{fa} = 10^{-3}$ for all values of δ for both 1 and 5 targets.

From figure 3 it is clear that for the single target case CS performs very close to the optimum MF. On the other hand, CS performs significantly better than DMF for small values of δ , because the effect of decimation in the DMF creates high target sidelobes, thus generating more false alarms at a given P_d , which becomes more apparent at high $SNRs$.

A. Grid mismatch errors

The simulations reported here were performed under ideal conditions, in the sense that no sources of error other than noise are present.

In practice there will be some error due to the fact that a true target position never falls exactly on the CS discrete model grid. However, it can be shown by analysis and simulation that

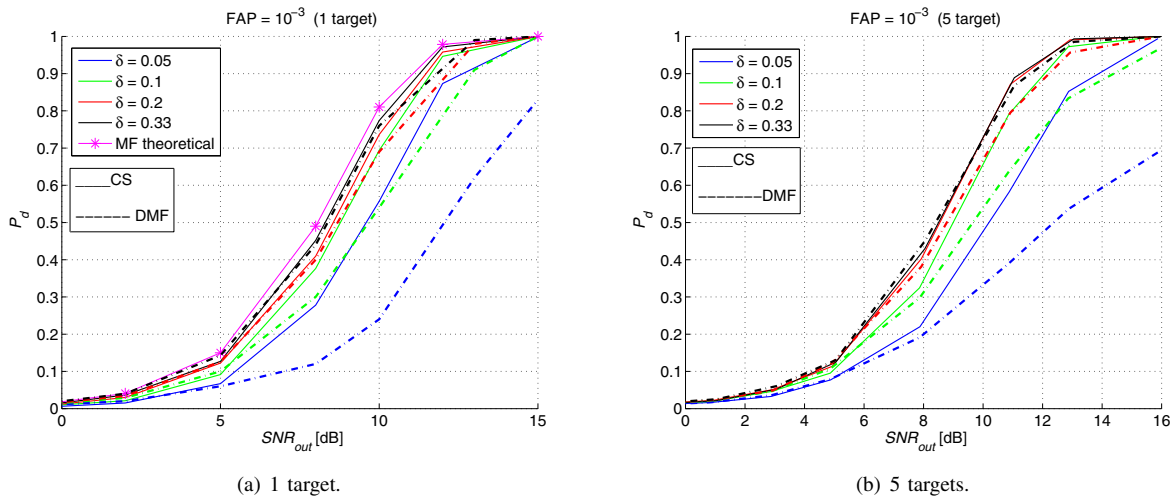


Fig. 3. P_d versus SNR . $FAP = 10^{-3}$. Solid lines: CS results. Dotted lines: DMF results.

the effect of the grid mismatch is similar to additional noise. Furthermore, just as in conventional matched filtering, the detected peak will be reduced by the fact that the target falls between samples. It is common practice to include a straddling loss in any radar system design, and in fact such a loss occurs in CS as well as in conventional linear filtering. An extensive discussion of grid mismatch is outside the scope of this paper; suffice it to show an example simulation, and to state that this aspect does not alter the general conclusions presented here. As shown in figure 4, the grid/target mismatch error has the effect of reducing the effective output SNR , and therefore also P_d decreases for a given FAP , both for matched filtering and for Compressive Sensing. In this example the number of compressed measurements is $M = 40$ and the grid mismatch error is $\Delta R/2$, which corresponds to the worst case scenario in which the target is exactly in the middle of two grid points. The ideal output SNR would be 15 dB (if there would be no grid error), however the loss in detection probability due to gate splitting can be converted into an equivalent loss in output SNR , which amounts for this example to approximately 3 dB. A practical way to compute the range gate loss is to average the ROC curves obtained for different amounts of grid mismatch. The figure also suggests that the straddling loss (present in both MF and CS) is much greater than the added 'grid' noise (which is only present in the CS case), by the fact that most of the loss is present in both MF and CS.

In e.g. [7] and [9] the authors propose to oversample the reconstruction grid to reduce 'grid' noise and straddling losses.

B. Coherent Processing

In many radar systems, several stages of coherent integration are used (e.g. range and Doppler) to achieve a satisfactory P_d or resolution. In this case, for instance, coherent integration of the range profiles over a Coherent Processing Interval (CPI) can be performed to improve SNR and detection capability. In conventional matched filtering, by coherent summation of P sweeps, the output SNR is improved by a factor of P . In

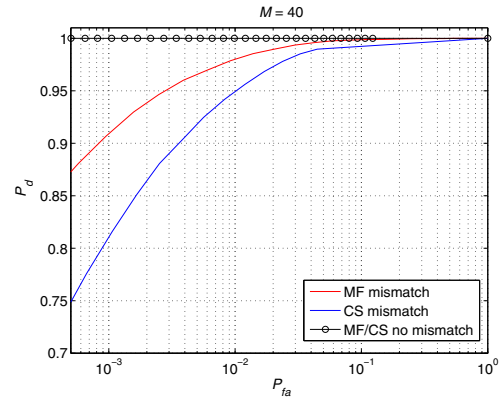


Fig. 4. ROC with $\Delta R/2$ grid mismatch error. Ideal MF output $SNR = 15$ dB (without grid error). $M = 40$.

Compressive Sensing however, due to the non linearity of the solution of equation (2), it is not obvious beforehand that the coherent summation can be performed, nor that it will increase the output SNR by the same factor. To investigate this aspect, the distribution of the reconstructed target amplitude and phase was also analyzed by means of simulations.

In order to perform coherent integration, the original signal phase has to be preserved. In figure 5 an example is shown of the 2 dimensional histogram of target amplitude and phase after noisy CS reconstruction. This behavior is consistent for all simulated cases, and it appears that amplitude and phase are independent and (mean) phase is preserved. Also the standard deviation of the estimated phase is equal for CS and DMF (0.183 radians in this example) and comparable to MF (0.180 radians). This behavior suggests that coherent integration can be performed after CS reconstruction just like in classical linear filtering.

As an example, in figure 6 the result of coherent integration is shown for the case $M = 50$, $SNR_{out} = 5$ dB and coherent integration of 20 sweeps. In this figure the real target is

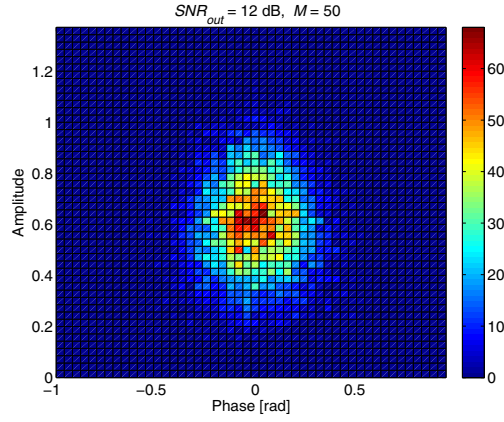


Fig. 5. 2 dimensional histogram of CS estimated target amplitude and phase. $SNR_{out} = 12$ dB, $M = 50$. True target amplitude is equal to 1 and true target phase is equal to 0.

positioned at 65 m range.

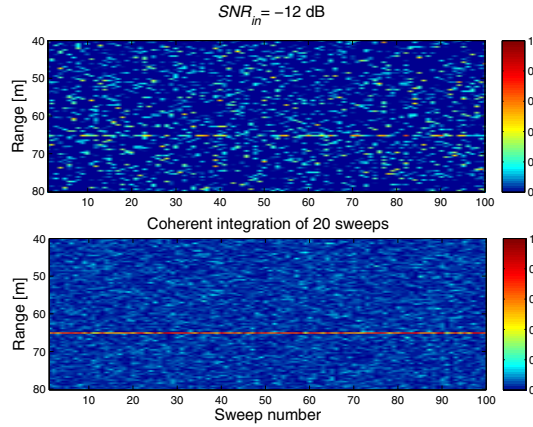


Fig. 6. Reconstructed signal with target at 65 m range. $SNR_{in} = -12$ dB, $M = 50$. Top: no coherent integration (only 100 sweeps are shown of the total 10000). Bottom: coherent integration of 20 sweeps (only 100 sweeps are shown of the total 500).

It is well known that, even at high $SNRs$, due to the soft thresholding operation which is used in most algorithms to solve equation (2) the CS estimated target amplitude is biased by an amount proportional to the threshold σ_{bpdn} ⁴. This behavior can also be seen in figure 5, where the estimated mean target amplitude is about 0.6 while the real target amplitude is 1. More importantly, if SNR is low, then the estimated amplitude of the target can be equal to zero with non-zero probability. When this happens, there is no way to improve any detection probability, as the target is simply lost. In such a scenario one should either use a very low threshold σ_{bpdn} , thus allowing more noise to be reconstructed and to suppress the extra noise later by integration or make

⁴For certain applications, such as imaging or clustering, it may be important to reduce the bias on the estimated amplitudes of detections. A possible way to do this is by applying least square estimation on the reconstructed non-zero CS samples, as already proposed in [15].

a statistical analysis and compute how many sweeps should be integrated to achieve a desired P_d , taking into account that the reconstructed target amplitude will be zero with a given probability. As an example in figure 7 the probability of having a reconstructed target amplitude equal to zero is shown versus SNR for different values of σ_{bpdn} for $M = 50$. From the ROC curves it appears that for this value of M the optimum value, in terms of ROC curve, for the BPDN threshold is 6σ . Referring to the same BPDN threshold in figure 7 it can be seen that e.g. for $SNR_{out} = 5$ dB, 35% of the time the reconstructed target amplitude is zero. This means that to achieve a specified improvement with coherent integration a larger number of sweeps in the CPI should be integrated compared to a matched filter output.

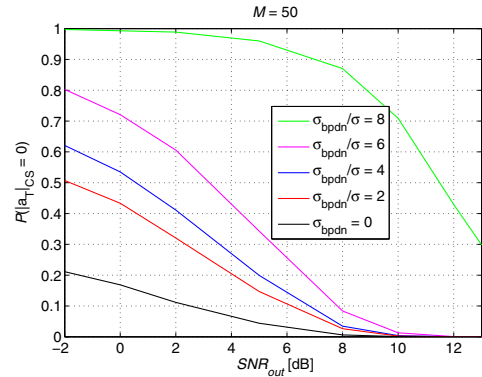


Fig. 7. Probability of having zero amplitude at target position using CS reconstruction versus SNR for $M = 50$.

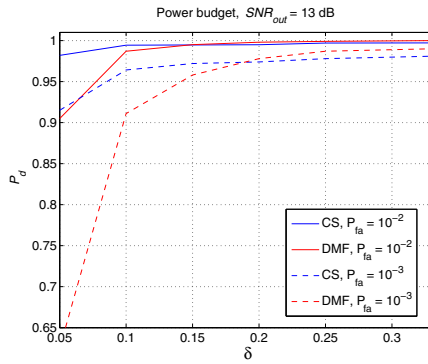
IV. CS POWER BUDGET

Using the ROC figures one can answer the question of how much compression can be applied with a given transmitted power (i.e., a fixed power budget), and what is then the P_d for a fixed FAP⁵.

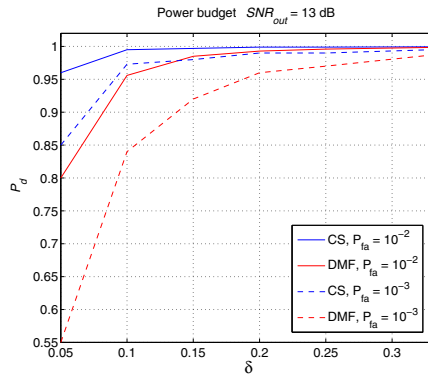
In figure 8 detection probability is shown versus δ for $SNR_{out} = 13$ dB for both 1 and 5 targets. As expected, for a fixed transmitted power, detection performance of the CS algorithm improves as M increases. On the other hand, for $\delta \geq 0.1$ the improvement is quite small with increasing M . Only when $\delta \leq 0.1$ the performance of CS starts to degrade significantly. However the DMF degrades even more than CS when δ decreases below 0.1.

From a system point of view, one can see from the ROC curves how transmit power can be traded against sample reduction. For a fixed P_d , it can be computed how much SNR increase (i.e. power increase) is required to compensate for a reduction of samples (M). When $\delta \leq 0.1$ this power increase becomes significant.

⁵Recall from the definition of SNR in section II-B that assuming constant transmitted power is equivalent to having equal SNR_{out} for all M (but different SNR_{in}).



(a) 1 target.



(b) 5 targets.

Fig. 8. Power budget for CS and DMF. P_d versus δ for $FAP = 10^{-2}$ (solid line) and 10^{-3} (dashed line). $SNR_{out} = 13$ dB.

V. CONCLUSION

In this paper detection performance of a Compressive Sensing based radar was investigated. The simulation results show that detection after CS reconstruction can closely approach classical detection performance, with fewer frequency samples. However selection of the BPDN threshold plays a significant role, and better performances in terms of ROC are achieved when the CS reconstruction is followed by a separate detector. Moreover, ideally CS does not produce target side lobes in the way that Decimated MF does, which improves FAP with respect to DMF for a fixed threshold. The ROC curves also allow a trade-off between transmit power and sample reduction. For example when the ratio of CS measurements to reconstructed samples is smaller than 0.1 (i.e. $\delta < 0.1$), maintaining a given probability of detection starts to require a significant power increase, both in 1 and 5 targets scenarios. Finally it was shown, that coherent integration after CS is possible, much like a conventional coherent radar processor provided that the reconstruction threshold is low enough to ensure a non-zero target amplitude.

ACKNOWLEDGMENT

The authors would like to thank Prof. J. Ender from Fraunhofer FHR, Germany, for the fruitful discussions.

REFERENCES

- [1] E. J. Candes, J. Romberg, and T. Tao, "Robust uncertainty principles: Exact signal reconstruction from highly incomplete frequency information," *IEEE Trans. Inf. Theory*, vol. 52, no. 2, pp. 489-509, February 2006.
- [2] E. Candes, and T. Tao, "Decoding by linear programming," *IEEE Trans. Inform. Theory*, vol. 51, no. 12, pp. 4203-4215, December 2005.
- [3] E. J. Candes, and T. Tao, "Near optimal signal recovery from random projections: Universal encoding strategies?," *IEEE Trans. Inf. Theory*, vol. 52, no. 12, pp. 5406-5425, December 2006.
- [4] D. L. Donoho, "Compressed sensing," *IEEE Trans. Inf. Theory*, vol. 52, no. 4, pp. 1289-1306, April 2006.
- [5] S.S. Chen, D.L. Donoho, and M.A. Saunders, "Atomic decomposition by basis pursuit," *SIAM J. Sci. Comput.*, vol. 20, no. 1, pp. 33-61, 1998.
- [6] R. Baraniuk, "Compressive sensing," *IEEE Sig. Proc. Magazine*, vol. 24, no. 4, pp. 118-121, July 2007.
- [7] J. H. G. Ender, "On compressive sensing applied to radar," *Elsevier Journal of Sig. Proc.*, vol. 90, no. 5, pp. 1402-1414, May 2010.
- [8] R. G. Baraniuk, and T. P. H. Steeghs, "Compressive Radar Imaging," *IEEE Radar Conference*, Waltham, MA, April 2007.
- [9] Y. Yu, A. P. Petropulu, and H. V. Poor, "MIMO radar using compressive sensing," *IEEE Journal of Sig. Proc.*, vol. 4, no. 1, pp. 146-163, February 2010.
- [10] M. A. Herman, and T. Strohmer, "High-Resolution Radar via Compressed Sensing," *IEEE Trans. on Sig. Proc.*, vol. 57, no. 6, pp. 2275-2284, June 2009.
- [11] A. C. Gurbuz, J. H. McClellan, and W. R. Scott, "Compressive sensing for Subsurface Imaging using Ground Penetrating Radar," *Journal of Sig. Proc.*, vol. 89, no. 10, pp. 1959-1972, October 2009.
- [12] Y. Wang, G. Leus, and A. Pandharipande, "Direction Estimation using Compressive Sampling Array Processing," *Proceedings of IEEE/SP 15th workshop on Statistical Signal Processing*, pp. 626-629, Cardiff, September 2009.
- [13] L. Anitori, M. Otten, and P. Hoogeboom, "Compressive Sensing for High Resolution Radar Imaging," *Proceedings of Asia-Pacific Microwave Conference 2010*, Yokohama, Japan, December 2010.
- [14] E. van den Berg and M. P. Friedlander, "Probing the Pareto frontier for basis pursuit solutions," *SIAM J. on Scientific Computing*, vol. 31, no. 2, pp. 890-912, November 2008.
- [15] E. Candes and T. Tao, "The Dantzig selector: Statistical estimation when p is much larger than n," *Ann. Statist.*, vol. 35, no. 6, pp. 2313-2351, 2007.
- [16] R. Tibshirani, "Regression shrinkage and selection via the lasso," *J. Roy. Stat. Soc. Ser. B*, vol. 58, no. 1, pp. 267-288, 1996.
- [17] L. Anitori, M. Otten, and P. Hoogeboom, "False Alarm Probability Estimation for Compressive Sensing Radar," *Proceeding of 2011 IEEE Radar Conference*, Kansas City, USA, May 2011.